Influence of Core Diameter on the 3-dB Bandwidth of Graded-Index Optical Fibers

Gnitabouré Yabre, *Member, IEEE*

***Abstract*—The frequency response and bandwidth of multimode silica glass fibers are investigated in this paper. The theoretical model incorporates both wavelength and modal effects including power coupling from random microbends. The 3-dBo bandwidth is examined through the study of the fiber transfer function which introduces the wavelength and modal effects as two separate filter functions. The formal derivation of the chromatic transfer function is analytical. On the other hand, the modal bandwidth is obtained by numerically solving the power flow equation in the frequency domain using the Crank–Nicholson method. As an application, the transfer function is illustrated and subsequently discussed with special focus spent on analyzing the influence of the fiber size in combination with the launching conditions. We show in particular that the larger the core, the greater the bandwidth potential of the fiber when operated under selective mode excitation. Some measurements are also carried out and excellent agreement between this model and data is achieved.**

***Index Terms*—Crank–Nicholson method, differential mode attenuation, dispersion, graded-index (GRIN) optical fibers, mode-coupling, optical communications, power flow equation.**

I. Introduction

PTICAL networking has become a major research topic currently driving much activities in the field of lightwave technology. Glass optical fibers (GOF's) do present more transmission capacity and lower attenuation than conventional physical media, thereby allowing communication signals to be transmitted at much higher rates over longer distances. This performance follows not only from the propagation of a single optical carrier over single-mode fibers (SMF's) operated in the lowest-loss windows (located around 850, 1300, and 1550 nm) but also from the emergence of erbium-doped fiber amplifiers (EDFA's) and upgrade technologies such as wavelength-division multiplexing (WDM). Single-mode GOF's are now widely used in many terrestrial and transoceanic communication links and these wide area network (WAN) applications are expected to keep on growing. The main objective of fiber-optic link operators is to extend the fiber coverage to smaller local area networks (LAN's) in the view of enabling the simultaneous handling of various services (voice, video, data) through all-optical systems. The problem of concern is that single-mode fibers that are widely installed in WAN links appear to be impractical for use within LAN's. As a matter of fact, the small core diameter (typically 10 μm) of SMF's would be incompatible with the manifold junctions, connectors, couplings that are often required in LAN's. The solution is given by multimode fibers (MMF's) that have large core diameters (50–1500 μm) to ease their connections and large numerical apertures (0.16–0.65 for GOF's) to allow for efficient couplings to semiconductor lasers.

Unfortunately, MMF's propagate a large number of modes having different velocities, thereby producing a signal response inferior to that of single-mode fibers. For standard 62.5/125 μm MMF's, the minimum bandwidths are only specified to be 200 and 500 MHz·km [1] in the 850 and 1300 nm transmission windows, respectively, under full-mode launch condition [2]. Even though such figures quite satisfy the information rate of a number of classical short-range links, it is clear that a 2-km long campus backbone cannot be realized for operation at the speed of Gigabit Ethernet. Until wavelength division multiplexing (WDM) technology becomes available and inexpensive, the potential MMF capacity for digital communication needs a greater exploitation to meet user need for higher data rates. To enable for such enhanced performances, several techniques have been proposed to overcome the intermodal dispersion. The main options include the use of microbending effects [3], [4], the design of so-called annealed MMF's [5], and the use of mode-filtering schemes [6], [7]. The first method has the main drawback that the bandwidth enhancement from microbends is accompanied by additional attenuation due to the coupling-induced loss. The main problem of the second alternative is that time is required to properly design a new generation of MMF's that can be mass produced, and the resulting cost will be inevitably high. Although these possibilities cannot be ruled out, for a near term implementation, only the upgrading can provide the lowest cost solution since the existing fiber plants need not be changed. For this reason, the selective-mode excitation technique is currently attracting much attention as a means of increasing the bandwidth-distance product [6], [7]. The motivation behind the present work is to contribute to a discussion concerning this alternative. The analysis presented in [7] was mainly focused on the study of standard 50/125 and 62.5/125 μm MMF's in the situation where the axis of the incident beam is shifted from the core center ("offset launch"), and little attention was given to the axial launching. Because the smallest number of modes can only be excited by positioning the beam spot against the core center, we believe that this method of excitation should potentially cause the smallest dispersion. Moreover, since a few low-order modes are involved, which propagate near the fiber axis, this technique can be expected to cause much less power loss in comparison to the offset launch.

In this paper, we explore the potential of the axial launching in greater detail. This work is achieved using a newly developed dispersion model as it appears that none of the predic-

Manuscript received October 6, 1999; revised January 17, 2000.

The author is with COBRA, Interuniversity Research Institute, Eindhoven University of Technology, EH 12.33, Eindhoven 5600 MB, The Netherlands.

Publisher Item Identifier S 0733-8724(00)03735-X.

tion tools reported in the existing literature incorporates the involved parameters together. The main parameters include the combined effect of material dispersion and source linewidth [8], [9], the launching conditions [7], and the mode-dependent parameters (i.e., propagation delay [8], attenuation [10], and the coupling coefficient [3], [4]). The 3-dBo cutoff bandwidth of the fiber is discussed through the study of the transfer function which introduces the wavelength and modal effects as two separate functions. The formal derivation of the chromatic transfer function is analytical, whilst the modal transfer function is obtained by numerically solving the power flow equation in the frequency domain. This calculation is followed by a clear evaluation of the total number of mode groups initially excited in the fiber. By examining this development the bandwidth behavior can be physically understood. Furthermore, the illustrative curves show how the parameters of the beam should be chosen to achieve a desired signal response. Special attention is spent on analyzing, for the first time, the influence of the core and outside diameters. We show in particular that the size of the core increases the bandwidth potential of the MMF under restricted mode launching condition. All computer simulations are based on studying high-quality silica glass fibers fabricated by Plasma Optical Fiber. Some measured results are also presented showing excellent agreement with theory.

II. Theory

We consider the class of circular symmetric graded-index (GRIN) fibers described by the refractive index profile

$$n(r,\lambda)=\begin{cases} n_1(\lambda)[1-2\Delta(\lambda)(r/a)^{\alpha}]^{1/2} & \text{for } 0\le r\le a \\ n_1(\lambda)[1-2\Delta(\lambda)]^{1/2} & \text{for } r\ge a \end{cases} \tag{1}$$

where r is an offset distance from the core center, λ is the wavelength (in free-space), α is the index exponent $(\alpha>0), n_1(\lambda)$ is the core peak index, $\Delta(\lambda)$ is the refractive-index contrast, and a is the core radius.

Multimode optical fibers described by (1) support a large but finite number of modes which are particular solutions of the Maxwell's equations. Guided modes propagating along the fiber are clustered into families in which modes have almost similar propagation constant. From the WKB analysis the propagation constant of mode groups can be derived analytically, which leads to [8]

$$\beta=2\pi\frac{n_1(\lambda)}{\lambda}\left\{1-2\Delta(\lambda)\left[\frac{m}{M(\lambda)}\right]^{2\alpha/(\alpha+2)}\right\}^{1/2} \tag{2}$$

where m stands for the principal mode number and $M(\lambda)$ is the total number of mode groups that can be potentially guided in the fiber. $M(\lambda)$ is given by [8]

$$M(\lambda)=2\pi a\frac{n_1(\lambda)}{\lambda}\left[\frac{\alpha\Delta(\lambda)}{\alpha+2}\right]^{1/2} \tag{3}$$

A. Dispersion Analysis

We consider a multimode fiber characterized by the α-class refractive index profile defined in (1) as linear in its input-output relationship [11]. In this case, we have recently shown that within some conditions that are expected to be satisfied in practice, the complex transfer function of such MMF's can be modeled by a product of two filter functions as follows [12]:

$$H_{\mathrm{MMF}}(\lambda_0,z,\omega)=H_{\mathrm{chromatic}}(\lambda_0,z,\omega)H_{\mathrm{modal}}(\lambda_0,z,\omega) \tag{4}$$

where $H_{\mathrm{chromatic}}(\lambda_0,z,\omega)$ and $H_{\mathrm{modal}}(\lambda_0,z,\omega)$ represent chromatic dispersion and modal dispersion, respectively. The parameters appearing in argument of both functions are the baseband angular frequency ω, the transmission wavelength λ_0, and the transmission length z.

Equation (4) expresses the latent idea that chromatic and modal dispersions are independent effects and can be evaluated separately. Under the assumption that the power spectral density of the driving source has a Gaussian lineshape with an rms linewidth σ_λ, the chromatic transfer function can be calculated exactly, yielding [13], [14]

$$H_{\mathrm{chromatic}}(\lambda_0,z,\omega)=\frac{1}{(1+i\omega/\omega_2)^{1/2}}\times\exp\left[-\frac{(\omega/\omega_1)^2}{2(1+i\omega/\omega_2)}\right] \tag{5}$$

in which ω_1 and ω_2 have been introduced as abbreviations for

$$\omega_1=-[\sigma_\lambda D_0(\lambda_0)z]^{-1} \tag{6}$$

$$\omega_2=\left\{\sigma_\lambda^2[S_0(\lambda_0)+2D_0(\lambda_0)/\lambda_0]z\right\}^{-1} \tag{7}$$

where $D_0(\lambda_0)$ is the modal velocity dispersion averaged over all guided modes and $S_0(\lambda_0)$ is the averaged dispersion slope. It is important to realize that for a system operated around a zero material dispersion wavelength, the chromatic effect is not necessarily negligible because of the presence of the dispersion slope. Therefore, this term cannot be systematically ignored even in the zero dispersion region. It is also worth noting that (5), (6) and (7) are the same as those describing chromatic dispersion in single-mode fibers. The difference for MMF's is only that averaged values have to be used for $D_0(\lambda_0)$ and $S_0(\lambda_0)$ in order to include the contribution of all guided modes. This causes the chromatic transfer function as defined in (5) to slightly depend on all parameters that determine the propagation, i.e., launch conditions, distributed loss and mode-coupling.

The modal transfer function involved in (4) is given by [12]

$$H_{\mathrm{modal}}(\lambda_0,z,\omega)=\frac{\int_{x_0}^{1}2xR(x,z,\omega)\,dx}{\int_{x_0}^{1}2xR(x,z,0)\,dx} \tag{8}$$

where $x_0=1/M(\lambda_0), x=m/M(\lambda_0)$ and $R(x,\lambda_0,z,\omega)$ is the modal power in Fourier domain. The numerator in the right hand side of (8) is a normalization factor representing the total power at position z. The modal power distribution is described by the following power flow equation which incorporates not

only modal delay but also distributed loss and mode-coupling effects [4], [15]

$$\frac{\partial R(x,\lambda_0,z,\omega)}{\partial z} = -[i\omega\tau(x,\lambda_0)+\gamma(x,\lambda_0)]R(x,\lambda_0,z,\omega) + \frac{1}{x}\frac{\partial}{\partial x}\left[xd(x,\lambda_0)\frac{\partial R(x,\lambda_0,z,\omega)}{\partial x}\right] \quad (9)$$

where $\tau(x,\lambda_0)$ is the modal delay per unit length, $\gamma(x,\lambda_0)$ is the modal attenuation and $d(x,\lambda_0)$ is the mode-coupling coefficient normalized to $M^2(\lambda_0)$.

B. Solutions of the Power Flow Equation

Equation (9) can be solved exactly using certain approximations [3], [4]. Here, we consider the more general situation where all the coefficients are mode-dependent. In that case, no simple analytical solutions are available and the modal transfer characteristics can be obtained only by using a numerical method. Before presenting the numerical procedure, let us first specify the functional forms of the mode-dependent parameters [i.e., $\tau(x,\lambda_0),\gamma(x,\lambda_0)$ and $d(x,\lambda_0)$] as well as the fiber launching conditions.

1) Mode-Dependent Parameters: The modal delay per unit length can be derived from (2) using the definition $\tau(x,\lambda) = -\lambda^2\beta'/(2\pi c)$ where the prime denotes the derivation with respect to wavelength and c is the speed of light in vacuum. The calculation leads to

$$\tau(x,\lambda) = \frac{N_1(\lambda)}{c}\left[1-\frac{\Delta(\lambda)[4+\epsilon(\lambda)]}{\alpha+2}x^{2\alpha/(\alpha+2)}\right] \times\left[1-2\Delta(\lambda)x^{2\alpha/(\alpha+2)}\right]^{-1/2} \quad (10)$$

in which $N_1(\lambda)$ is the group index and $\epsilon(\lambda)$ is the profile dispersion parameter, respectively, given by

$$N_1(\lambda) = n_1(\lambda) - \lambda n_1'(\lambda) \quad (11)$$

$$\epsilon(\lambda) = \frac{-2n_1(\lambda)}{N_1(\lambda)}\frac{\lambda\Delta'(\lambda)}{\Delta(\lambda)}. \quad (12)$$

In case the weak guidance rule is sufficiently satisfied, formula (10) can be approximated by [8]

$$\tau(x,\lambda) = \frac{N_1(\lambda)}{c}\left[1+\Delta(\lambda)C_1(\lambda)x^{2\alpha/(\alpha+2)} +\Delta^2(\lambda)C_2(\lambda)x^{4\alpha/(\alpha+2)}\right]+\ldots \quad (13)$$

in which

$$C_\ell(\lambda) = \frac{(2\ell-1)\alpha-2-\ell\epsilon(\lambda)}{\ell(\alpha+2)} \quad \text{with } \ell=1,2. \quad (14)$$

It should be mentioned that it is the differences in modal delay (differential mode delay, DMD) that determines the intermodal dispersion. The constant term in (13) leads to an overall $\exp(-i\omega zN_1/c)$ factor to the complex transfer function and can be ignored in frequency response simulations.

The modal attenuation is incorporated in the model by fitting a proper function to the measured data. For this the following functional expression is proposed as approximation

$$\gamma(x,\lambda) = \gamma_0(\lambda) + \gamma_0(\lambda)I_\rho\left[\eta(x-x_0)^{2\alpha/(\alpha+2)}\right] \quad (15)$$

where $\gamma_0(\lambda)$ is the attenuation of low-order modes, I_ρ is the ρth-order modified Bessel function of the first kind, and η is a weighting constant. Of course, as in the case of modal delay, it is the difference in modal attenuation (differential mode attenuation, DMA) that determines the influence of the distributed loss. The first term in (15) leads to an overall factor $\exp[-\gamma_0(\lambda)z]$ to the solution and can be dropped. To obtain the numerical values of the DMA parameters, we have fitted (15) to the measured data presented in [16], which yielded $\rho = 9$ and $\eta = 7.35$.

Finally, the mode-coupling coefficient needs to be specified to proceed to the solutions of the power flow equation. The coupling between guided modes may result from multiple origins including internal imperfections as well as external perturbations. Consequently, it is an impossible task to evaluate the coupling phenomenon in the general case and one can succeed only through simplifying assumptions. Internal sources of mode-coupling may be the consequences of core noncircularity [17], crookedness in the lie of the fiber axis or refractive index fluctuations [18] caused by the fiber fabrication process. In principle, in modern glass fibers,the influence of the core diameter variations due to the fiber fabrication process should be negligible because those perturbations should extend over many centimeters, so that the phase matching condition is unsatisfied for modes belonging to different mode groups to exchange energy. On the other hand, because we deal with modern silica glass fibers made on using the high-performance PCVD method, we will also neglect the effect of refractive index variations. In other words, we will consider only random microbends caused by external forces to be the most dominant source of mode-coupling. A valuable study of this subject was previously presented by Olshansky [4]. We adopt here the same approach together with the selection rules of next neighboring mode group approximation, but we modify the form of the curvature spectrum to bring in the fiber external diameter [19]. In so doing, we found the following functional expression for the normalized mode-coupling coefficient

$$d(x,\lambda) = C_s\left(\frac{h}{b}\right)^2\left(\frac{a}{b}\right)^4\left[\frac{\alpha+2}{\alpha\Delta(\lambda)}\right]^3 x^{-2q} \quad (16)$$

with

$$q = 2(\alpha-3)/(\alpha+2) \quad (17)$$

where C_s is the mode-coupling constant, h is the rms height of the deformation and b is the total radius of the fiber.

To allow for computation, numerical values are required for the coupling parameters (C_s,h). For this, we formally set h to 1 μm and choose C_s such a way that the predicted attenuation at a given transmission length coincides with the measurement. We obtained $Cs = 6.5\ 10^{-5}$ km^{-1} which quite yields the 1.24

dB/km value supplied by Plasma Optical Fiber for a 93/125-μm fiber operated at the 1300 nm wavelength.

From (16), it can be noticed that for two different fibers drawn such a way that the ratio a/b remains constant, the one having the largest outside diameter will be less susceptible to microbending. On the other hand, if the fiber size is maintained to a constant value, the mode-coupling coefficient increases with larger core. Another comment that can be made from the above relations is that for large values of α, the parameter q is positive, which causes the coupling coefficient to increase with decreasing x. In the step-index case ($\alpha = \infty$), in particular, $q = 2$ and accordingly $d(x, \lambda)$ varies inversely with x^4. This demonstrates that low-order modes are more strongly coupled than high-order modes in step-index fibers. The result is the converse in the nearly parabolic-index version. This difference in behavior between the two types of profiles was previously confirmed by measurements [20].

2) Launching: A variety of light-coupling methods can be applied to multimode fibers [6], [7]. For the present application, we consider two cases, namely, the uniform launching and the axial excitation with a Gaussian input beam. In the former case, the initial power distribution is by assumption the same for each mode and can be formally set to unity. In the latter case, the mode excitation can be simulated by computing the launching efficiency as the overlap integral of the electrical field of each fiber mode with the electrical field of the incident light. Strictly speaking, this calculation should be carried out for the proper refractive index profile of the fibers in consideration. But, this is not an easy task since the modal fields can be determined analytically in terms of known functions only for $\alpha = 2$ and $\alpha = \infty$. However, as long as the refractive index remains nearly parabolic, as it is the case here, the distribution of the initial power is not expected to differ significantly from that of the perfectly parabolic profile. It is therefore appropriate to use the results of overlap integral calculation displayed in [21], [22]. We equally assume that the fiber axis is well aligned with the beam axis, and that its end surface is well positioned in the focal plane.

Together with the power distribution, the initial modal distribution plays a large part in the determination of the signal response of the fiber. Even though the number of initially excited modes is not directly involved in the dispersion model, its derivation as a function of the beam parameters should help to physically understand the bandwidth behavior. More importantly, such a development can provide a veritable theoretical basis for a more controlled choice of the input conditions during a real implementation of the selective-mode excitation. Therefore, we will quantitatively evaluate the initial mode group distribution when the fiber is axially launched with a Gaussian beam.

Let us consider a light ray entering the fiber at incident angle $\theta_{i,r}$ and propagating at an angle θ with respect to the fiber axis as explained in Fig. 1(b). We have the following relation for the axial propagation constant of that ray

$$\beta = \frac{2\pi}{\lambda} n(r, \lambda) \cos(\theta). \tag{18}$$

By taking (1) into account and introducing the Snell–Descartes law

$$n_i \sin(\theta_{i,r}) = n(r, \lambda) \sin(\theta) \tag{19}$$

where n_i is the refractive index of the medium in which the incident ray is propagating ($n_i \simeq 1$ for air), (18) becomes

$$\beta = 2\pi \frac{n_1(\lambda)}{\lambda} \left[1 - 2\Delta(\lambda) \left(\frac{r}{a}\right)^{\alpha} - n_1^{-2}(\lambda) \sin^2(\theta_{i,r})\right]^{1/2}. \tag{20}$$

Equating expressions (20) and (2) shows that the principal mode number corresponding to the propagated ray is given by

$$m = M(\lambda) \left\{ \left(\frac{r}{a}\right)^{\alpha} + [2n_1^2(\lambda)\Delta(\lambda)]^{-1} \sin^2(\theta_{i,r}) \right\}^{(\alpha+2)/(2\alpha)}. \tag{21}$$

The axial launching of the fiber by a Gaussian beam is schematically described in Fig. 1(a) where w represents the spot radius. It should be mentioned that Gaussian-shaped beams can readily be obtained from semiconductor lasers using classical projection means (e.g., lens doublet). In such a launch technique, the highest order mode group is excited by the plane-wave component striking the fiber input surface at the maximal offset distance w from the core center and at the maximal numerical aperture $\sin(\theta_{i,w})$. The latter can be viewed as the minimum between the numerical aperture (NA) of the incident beam and the fiber local NA at the lateral distance w. This approach is correct since our theory approximates guided modes by a continuum [12].

The numerical aperture of the Gaussian beam is approximately given by the relation $\lambda/(\pi w)$. For $\lambda = 1300$ nm and $w = 3\,\mu$m, for example, we obtain an NA of 0.14, which is less than the NA of current glass fibers (0.16–0.65). Accordingly, we can reasonably assume that for relatively large spots, the NA of the Gaussian beam is smaller than the local NA at w. In that case we have $\sin(\theta_{i,w}) = \lambda/(\pi w)$, according to the above definition. Hence, by substitution into (21) and denoting the number of excited mode groups by $M_{\rm gb}$, we obtain

$$M_{\rm gb} = M(\lambda) \left\{ \left(\frac{w}{a}\right)^{\alpha} + \left[2\pi^2 n_1^2(\lambda)\Delta(\lambda)\right]^{-1} \left(\frac{\lambda}{w}\right)^2 \right\}^{(\alpha+2)/(2\alpha)}. \tag{22}$$

Inspection of relation (22) shows that the number of excited mode groups goes to infinity when w approaches zero or when w goes to infinity. It should be kept in mind, however, that $M_{\rm gb}$ must not exceed the maximum number of mode groups imposed by waveoptics and expressed in (3). More precisely, the input light will excite all the modes supported by the fiber if the beam overfills the core region or if it forms a small enough spot. Between the two situations, it is noteworthy that an optimum operation point exists for which a few modes as possible can be excited. The optimal spot radius that we will denote by $w_{\rm opt}$ is obtained by solving $\partial M_{\rm gb}/\partial w|_{w_{\rm opt}} = 0$, which yields

$$w_{\rm opt} = \frac{1}{[\alpha\Delta(\lambda)]^{1/(\alpha+2)}} \left[\frac{\lambda a^{\alpha/2}}{\pi n_1(\lambda)}\right]^{2/(\alpha+2)}. \tag{23}$$

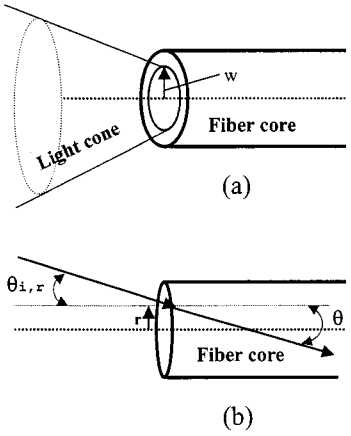

Fig. 1. Description of the launching. (a) Geometry of fiber excitation with an axial Gaussian beam and (b) ray trajectory.

Formula (23) is well-known from waveoptics-based calculations in the particular case of parabolic index fibers ($\alpha = 2$). Thus, $w_{\rm opt}$ was usually considered to be the spot radius of the beam that excites only the fundamental modes. However, it is anticipated that the matched Gaussian beam does excite two mode groups and not only one, regardless of the core diameter. This will be more appreciated through illustrative curves but can readily be verified by inserting (23) into (22) for $\alpha = 2$. This corresponds to six excited modes when taking the two-fold degeneracy of the mode groups into account. So, in contrast to the previous suggestions, this result quite demonstrates, that one mode group cannot solely be launched with a central Gaussian beam, even though in practice the fundamental modes will be maximally excited. This finding gives the explanation why the calculated optimum bandwidth of a standard 62.5/125-μm fiber at 1310 nm was found to be relatively small (10 GHz) [7]. If the fundamental modes were excited alone the fiber would have much behaved like the corresponding single-mode version and the bandwidth would have been several times or even an order of magnitude larger than the obtained 10 GHz, owing to the small material dispersion around the wavelength of measurement. The recorded small value means that the fiber response was additionally influenced by modal dispersion due to the presence of the second-order mode family.

The discrepancy between ray optics and wave optics is to be connected with the fact that Hermite-Gaussian and Laguerre-Gaussian mode fields are often used in the derivation of the overlap integrals, which results in nonzero coupling efficiencies only for odd values of the principal mode number m [22]. The problem is that the Hermite–Gaussian and Laguerre–Gaussian modes follow from the assumption of an infinitely extended square-law medium. This theory that regards the core as an unbounded region is not very realistic for a real fiber surrounded by a cladding, so "even" modes should practically carry some energy as well. For this reason, the Hermite–Gauss and Laguerre–Gauss approach should not, in a strict sense, be used in the dispersion model. Instead, the overlap integrals should be computed numerically from the Maxwell's equations in order to include the contribution of every propagated mode. However, because the mode-continuum approximation is presumed to be valid in our model [12], the error involved using the simplified representation by Hermite–Gaussian or Laguerre–Gaussian modal fields should not be significant. It is therefore convenient to adopt the calculation results of [21], [22].

3) Numerical method: The numerical integration consists of discretizing the x and z variables to form a rectangular lattice. At each point (i,k) of the grid the derivatives are approximated by an appropriate finite difference which determines the choice of method. A variety of such schemes are given in the literature. Here, we will adopt the Crank–Nicholson implicit procedure which yields a stable solution that converges more rapidly than ordinary difference methods [16], [23]. For this, let h_x and h_z be the segmentation steps of the variables x and z, respectively. The power flow equation with $R(x,\lambda_0,z,\omega)$ can be replaced by a set of finite-difference equations with $R_{j,k} = R(x_j,\lambda_0,z_k,\omega)$ where $x_j = x_0 + jh_x$ and $z_k = kh_z$. Using the Crank–Nicholson implicit scheme, (18) is transformed into

$$\begin{aligned} A_jR_{j-1,k+1} + B_jR_{j,k+1} + C_jR_{j+1,k+1} \\ = D_jR_{j-1,k} + E_jR_{j,k} + F_jR_{j+1,k} \end{aligned} \tag{24}$$

with

$$\begin{cases} A_j = -h_zd_j/h_x^2 \\ B_j = 2 + h_z(i\omega\tau_j + \gamma_j) + h_z(x_{j+1}d_{j+1} + x_jd_j)/(x_jh_x^2) \\ C_j = -h_zx_{j+1}d_{j+1}/(x_jh_x^2) \\ D_j = -A_j \\ E_j = 2 - h_z(i\omega\tau_j + \gamma_j) - h_z(x_{j+1}d_{j+1} + x_jd_j)/(x_jh_x^2) \\ F_j = -C_j \end{cases} \tag{25}$$

where

$$\begin{cases} d_j = d(x_j,\lambda_0) \\ \tau_j = \tau(x_j,\lambda_0) \\ \gamma_j = \gamma(x_j,\lambda_0). \end{cases} \tag{26}$$

The unknowns $R_{j,k}$ can be computed from (24) if the boundary conditions are specified. For this, our choice is the following:

$$\begin{aligned} \frac{\partial R(x_0,\lambda_0,z,\omega)}{\partial z} &= -(i\omega\tau_0 + \gamma_0)R(x_0,\lambda_0,z,\omega) \\ &\quad + M_0d_0\left[\frac{\partial R(x,\lambda_0,z,\omega)}{\partial x}\right]_{x=x_0} \end{aligned} \tag{27}$$

$$R(x,\lambda_0,z,\omega) = 0 \quad \text{for } x > 1. \tag{28}$$

The boundary condition (27) stands for the propagation equation of the fundamental modes, while the upper boundary condition (28) is established by considering that leaky modes do not transport significant power, which should be a realistic assumption. It is worth mentioning that once the $R_{j,k}$ are determined, the modal transfer function can be derived by approximating (8) by any suitable numerical integration method. Here we have used Simpson's rule in the frequency response simulations. The results will now be shown and discussed.

III. Results and Discussion

We analyzed the dispersion characteristics of ternary GRIN fibers with a GeO_2–F–SiO_2 core and F–SiO_2 cladding. These

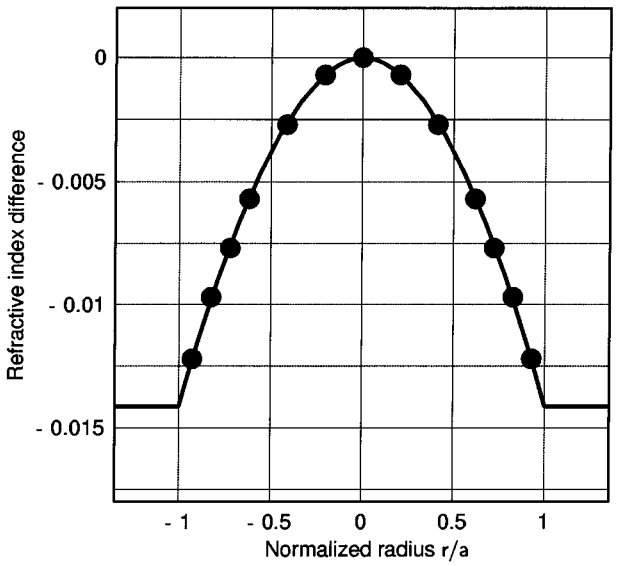

Fig. 2. Refractive-index profile of the studied glass fibers: (•••) Measurement on PCVD preform, (———) Best fitted index difference $n(r,\lambda_0) - n(0,\lambda_0)$ with $\alpha = 1.9$.

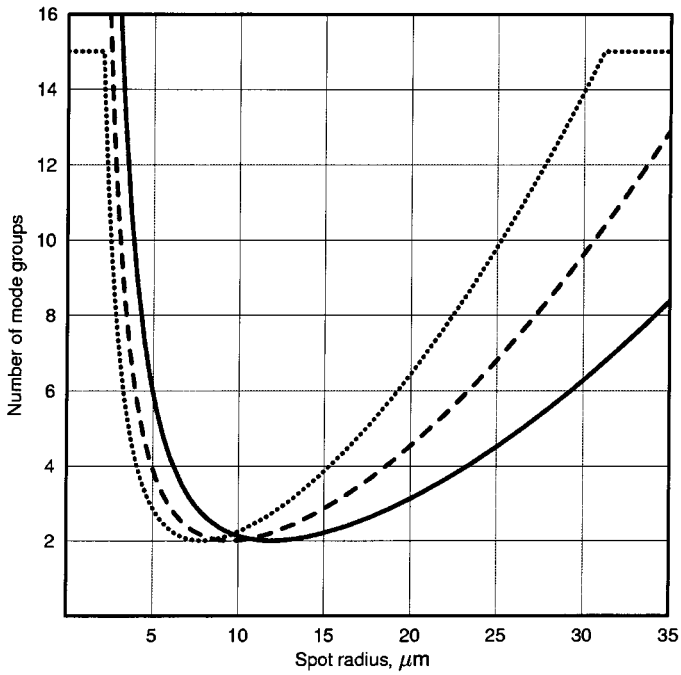

Fig. 3. Total number of excited mode groups as a function of spot radius for varying core diameter: (———) $2a = 148$ μm, (– –) $2a = 93$ μm, (· · · · · ·) $2a = 62.5$ μm.

fibers are fabricated by Plasma Optical Fiber by the high-performance PCVD method. A small amount of fluorine (0.004 mol-%) is uniformly doped over the core and cladding regions. The core center has a 13.5 mol-% of germanium which is gradually decreased in the lateral direction to form the grading. To enable computer evaluations, it is assumed that the refractive indices of the core and cladding materials follow three-term Sellmeier functions of wavelength [24]. These choices of parameters yield a numerical aperture $\mathrm{NA} \simeq 0.2$ in the 1300-nm wavelength region, and the core exhibit a refractive index profile that can be approximated with an α-factor close to 1.9 (see Fig. 2). On the other hand, the material dispersion versus wavelength characteristic shows a zero crossing near 1300 nm and a -94·ps/nm·km value at 850 nm. The dispersion slopes at the same wavelengths are found to be 0.1 and 0.4 ps/nm^2·km, respectively. For the rest of the work, the 1300 nm region will be uniquely considered. The frequency responses as embodied by (4) are simulated based on three different fibers spooled on separate 30 cm-drums and measuring 2014 m in length and having 62.5/125, 93/125, 148/200 μm core/cladding diameters, respectively.

The number of mode groups excited by an axial Gaussian beam is reported in Fig. 3 as a function of the spot radius, for the three different fibers under consideration. It can be observed first that projecting a small spot onto the center does not necessarily constitute a restricted launching, but a large number of modes, or even all the modes that can potentially propagate, could be excited. This is so because the local numerical aperture is the highest in the core center and corresponds to the very numerical aperture of the fiber. In other words, the positioning of a small beam spot against the center of the core should lead to the same bandwidth than the overfilling of the core region with a large spot.

In accordance with earlier indication, each characteristic in Fig. 3 is seen to exhibit a minimum corresponding to two mode groups, regardless of the size of the core. More importantly, the effect of the core diameter can be analyzed in the same figure by comparing the curves by pair. The presence of crossover points can be noticed. Because the number of guided modes determines the level of modal dispersion, these regions mark the points from which the considered fibers will practically show inverse bandwidth performance. More precisely, for an incident beam having a spot radius lower than the crossover value, the largest core sample will propagate more modes than the thin-core one and therefore will exhibit less bandwidth. This result will be the converse if the beam spot radius is larger than the crossover value. Of course, these qualitative predictions should hold true only for transmission distances not exceeding the characteristic coupling length. It should equally be noticed that because the fiber response depends not only on the number of guided modes but also on the power distribution and further parameters as indicated earlier, the crossover points may slightly shift in the bandwidth domain. The results of Fig. 3 will be more appreciated by reference to further curves.

Fig. 4 shows the frequency responses of a $93/125$ μm fiber at transmission length of 2014 m. The simulations are made for two types of launching, that is, the SMF-to-MMF butt-joining and the complete mode filling showing the influence of mode-coupling. In the former case, measured data are also reported. The driving source was an SMF-pigtailed module employing a classical Fabry–Perot laser emitting at the central wavelength of 1308 nm. The measured frequency response was recorded using a 3-GHz network analyzer (HP 8702A). From Fig. 3, the following observations can be made. First, we see that in the SMF-to-MMF launch case for which both experiment and theory are compared, the characteristics show excellent agreement. Second, the results confirm that more bandwidth can be

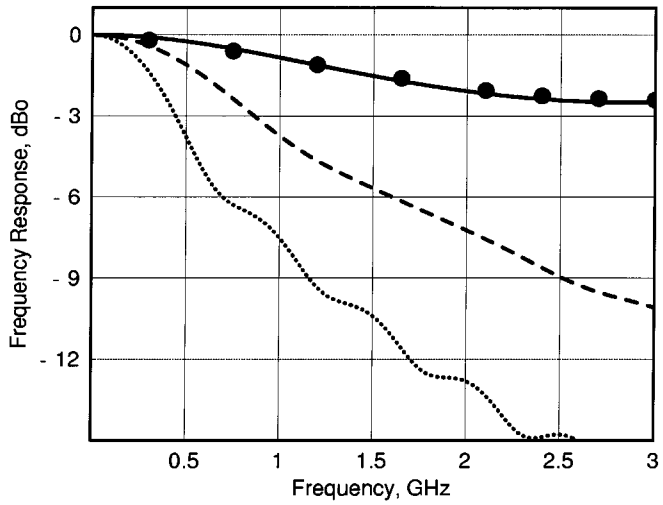

Fig. 4. Frequency responses of the 93/125 μm fiber at 1308 nm wavelength under two different excitation conditions: (———) SMF-to-MMF launching (theory), (• • •) SMF-to-MMF launching (experiment), (– –) Theoretical simulation under overfilled launching (OFL) including distributed loss and random perturbation effect, (· · · · · ·) Theoretical simulation under OFL excluding random perturbation effect.

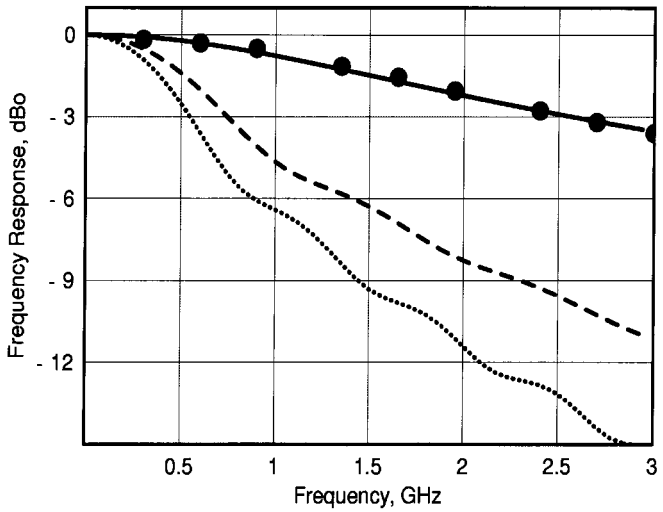

Fig. 5. Frequency responses of the 148/200 μm fiber at 1308 nm wavelength under two different excitation conditions: (———) SMF-to-MMF launching (theory), (• • •) SMF-to-MMF launching (experiment), (– –) Theoretical simulation under overfilled launching (OFL) including distributed loss and random perturbation effect, (· · · · · ·) Theoretical simulation under OFL excluding random perturbation effect.

gained by mode-coupling. This improvement follows from the fact that the mixing process forces the total light energy to travel at an overall speed that is an average of the modal group velocities [25]. Since no extra mode is excited during propagation, the average speed is less than that of an otherwise similar fiber having no mode mixing. This explains the higher signal response. Another observation that can be made from Fig. 4 is that the full-mode excitation yields a much lower frequency response with respect to that of the SMF-to-MMF launching. This behavior remains true in the presence of random perturbations. The 3-dBo bandwidth is found to be 0.87 GHz in the full launch case and 9.10 GHz (not shown in Fig. 4) in the SMF-to-MMF launch case, which is far beyond the detection limit of the measurement system. These results clearly demonstrate that the input conditions play a much more significant role in providing a large bandwidth than the random perturbations combined with a normal excitation. Intentional microbends could be built in the fiber to increase the coupling strength and rise the potential signal response, but this will cause extra power penalty as a result of the tradeoff relation between bandwidth and coupling-induced losses.

In order to analyze the influence of the core/cladding diameters, we have reported the frequency responses of the 148/200 μm sample in Fig. 5 where the curves have the same significance as in Fig. 4. Again, a good agreement is obtained between simulation and measurement for the SMF-to-MMF launching case. The corresponding 3-dBo bandwidth is 2.23 GHz, whilst it is found to be 0.75 GHz for the complete and uniform mode excitation regime. Compared to the previous values, we see that the bandwidth for the same launching condition is reduced with higher diameter. This result is quite in agreement with the theoretical studies. Indeed, in the full-mode launch case the bandwidth reduction follows from (16) which shows that the coupling strength reduces with larger outside diameter. In the SMF-to-MMF launch case the reduction in the bandwidth is to be connected with the larger number of excited modes. This interpretation is in line with the solid curve in Fig. 3 since the SMF beam results in a spot radius of 6 μm, approximately.

It is convenient to verify further in terms of fiber bandwidth the initial modal distribution as displayed in Fig. 3. For this, a series of frequency responses were simulated showing the effects of the spot radius and that of the core diameter, separately. Some of these results are reported in Figs. 6 and 7. The upper part of Fig. 6 plots the dependence of the standard fiber bandwidth on launch spot radius, whilst Fig. 7 plots the frequency responses of the three fibers for a constant spot radius of 19 μm. We see that the shape of the curve in Fig. 6 is consistent with the shape of the dotted characteristic in Fig. 3. In particular, the optimum spot radius providing the highest bandwidth is found to be 7.8 μm, which coincides with the optimum operation point in Fig. 3. From Fig. 6, it can also be noticed that the optimum spot radius is not critical but its value can vary over a certain range without significantly altering the bandwidth performance. This is of interest if a practical implementation of this technique is to be realized.

Fig. 7 also reflects quite well the modal picture shown in Fig. 3. Indeed, we see that the 3-dBo bandwidth increases with larger core. We found it useful to compare the highest 3-dBo bandwidth in Fig. 7 (16 GHz) with that of the standard 62.5/125 μm fiber under optimal launching. The latter can be derived either from the upper part of Fig. 6 or from the lower part which shows the full optimum frequency response. The result is 8 GHz, which corresponds to a twofold reduction with respect to the bandwidth of the 148/200 μm sample in Fig. 7. This clearly demonstrates that the large-core fiber has more bandwidth potential. The physical reasons behind this trend are not thoroughly understood yet. We believe that this should mainly result from the fact that the difference in propagation constant between next-neighboring mode groups

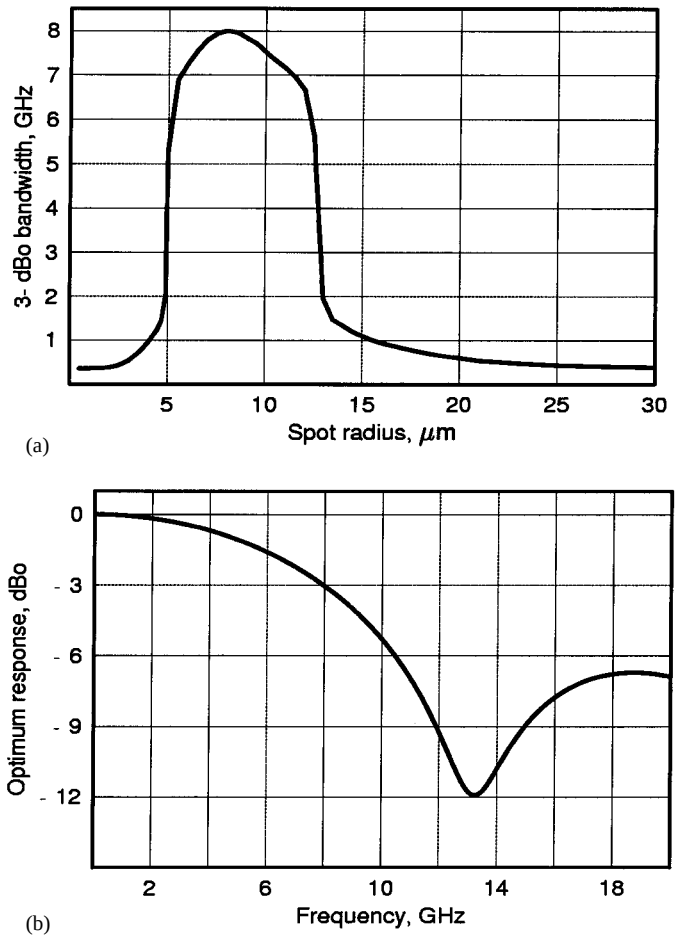

Fig. 6. Characteristics of the 62.5/125 μm fiber at 1308 nm wavelength: (a) dependence of bandwidth on beam spot radius and (b) optimum frequency response.

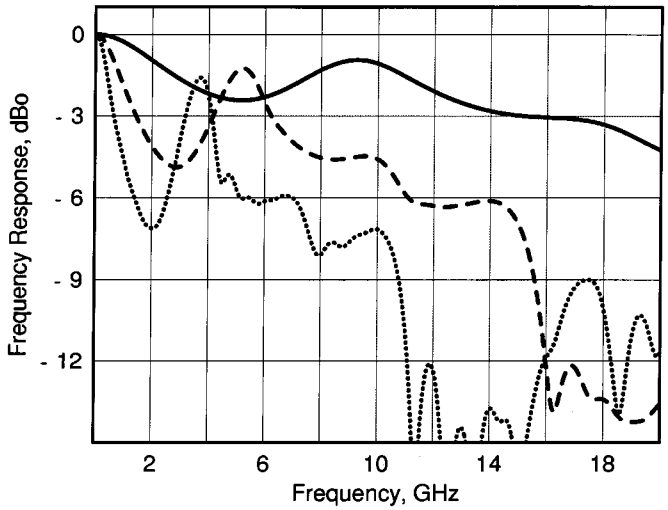

Fig. 7. Theoretical frequency responses of three different fibers at 1308 nm wavelength for a constant spot radius of 7.8 μm: (———) $2a = 148\ \mu$m, (– –) $2a = 93\ \mu$m, (· · · · · ·) $2a = 62.5\ \mu$m.

is inversely proportional to the core diameter [26] and therefore reduces as the core is enlarged. It can be noticed, however, that a low-frequency dip sometimes appears in the frequency response. The presence of the dip was already slightly apparent from Fig. 4 (in the SMF-to-MMF launch case). It may affect a broad-band transmission performance and therefore may cause the limitation of the potential bandwidth to values much lower than the the 3-dBo cutoff frequency available. Future work will be done to investigate this phenomenon in more detail.

To end this discussion, we believe that the axial launch into the core provides a promising alternative for enhancing the bandwidth-distance performance of LAN's wired with multimode fibers. It is clear from the above study that under selective operation, MMF's can transmit much larger bit rates over longer distances than usual. In particular, using this technique, the speed and distance requirements of Gigabit Ethernet could easily be met. As far as restricted-mode launching is concerned we dare say that the thick-core fiber is the most appropriate. As we saw, its bandwidth is not necessarily lower than that of an otherwise similar fiber but having thinner core. Instead, the forgoing work shows that the large-core fiber can exhibit equal or even higher response than the thin-core one if the launch conditions are properly chosen. On the other hand, the size of the fiber is useful for minimizing the microbending effect, thereby allowing for a large coupling length. The easy connectorization of large-core fibers can also be mentioned as an additional advantage. The main worry concerns the modal noise immunity of such selective systems and eventually their higher sensitivity to mechanical agitation compared to those using the classical overfilled launching. The latter problem can be prevented by properly optimizing the input connector and by reinforcing the cabling. The modal noise aspect is not investigated yet, but we are of the opinion that the immunity should not degrade significantly. It may even rather improve for the following reasons. The light energy will essentially be contained in a few low-order modes guided near the fiber axis. In that case, indeed, Saijonmaa and Halme have shown that the modal noise may be dramatically reduced at fiber-fiber joint [22]. On the other hand, because low-order modes have the smallest divergence, the outgoing beam will be easier to image, thereby minimizing its susceptibility to produce modal noise on the receiver side. It is also worth mentioning that if the modal noise cannot be completely suppressed, the resulting residual power penalty can be compensated by the greatly reduced dispersion penalty that will necessarily follow from the large bandwidth enhancement. As a result of this study, we propose that, because the size of the input beam spot determines the selective operation, this parameter be considered, from now on, as a figure of merit for optical transmitters that are to be used in MMF networks.

IV. Conclusion

The dispersion behavior of GRIN silica-glass fibers is theoretically and experimentally presented. The theoretical results are obtained using a newly-developed dispersion model which includes both distributed loss and mode-coupling effects. In this model the fiber frequency response is described as a product of two separate functions regarded as frequency responses caused by chromatic and modal dispersions.

The analysis of computer simulations and measurements are mainly focused on the influence of the core/outside diameters

in conjunction with the input conditions. It is emerged that the latter parameter plays a much more significant role in minimizing the intermodal dispersion than the mode-coupling from random perturbations. The results also show that the size of the fiber core does not constitute an obstacle to achieving a low dispersion. On the contrary, this study quite demonstrates that thick-core MMF's may exhibit larger bandwidth than thin-core ones if the input conditions are properly chosen. Because thick-core fibers additionally present little sensitivity to microbending and also because they are easier to connect, we believe that they are the best appropriate if a selective-mode excitation technique is to be implemented.

Let us mention *a posteriori* that the selective-mode launch which consists of initially coupling energy only into a given subset of propagating modes should not be too difficult to achieve in practice. As we saw, the direct butt-joining of an SMF to the MMF could lead to a selective-mode excitation depending on the core diameter. This is convenient because most commercially available optical transmitter modules terminate with single-mode fiber pigtails. On the other hand, for MMF's with arbitrary cross sections, suitable input spots can generally be obtained from SMF's and semiconductor lasers using conventional projection means such as lens doublets. In other words, there is no apparent tradeoff of having to control the mode-launch versus the bandwidth gain in larger core region. More work will be done in future to complete the evaluation of the potential of large core MMF's under selective-mode operation.

ACKNOWLEDGMENT

This work was done within the framework of the Dutch research project IOP Electro-Optics ongoing in the COBRA research institute, Eindhoven University of Technology. Continuous and helpful discussions with Prof. G. D. Khoe, Dr. H. de Waardt, and Ir. H. P. A. van den Boom are acknowledged. The author would equally like to thank Plasma Optical Fiber for making the fibers and for supplying his research group with samples. He also acknowledges helpful discussions with Dr. T. Breuls, Ir. G. Kuyt and Ir. M. de Fouw (from Plasma Optical Fiber) during the course of this study.

REFERENCES

[1] "Information Technology-Generic Cabling for Consumer Premises,", ISO/IEC 11 801: 1995 (E).
[2] "Mode Scrambler Requirements for Overfilled Launching Conditions to Multimode Fibers,", EIA/TIA 455-54A.
[3] D. Gloge, "Impulse response of clad optical multimode fibers," *Bell Syst. Tech. J.*, vol. 52, pp. 801–817, 1973.
[4] R. Olshansky, "Mode coupling effects in graded-index optical fibers," *Appl. Opt.*, vol. 14, pp. 935–945, 1975.
[5] J. Nishimura and K. Morishita, "Changing multimode dispersive fibers into single-mode fibers by annealing and guided mode analysis of annealed fibers," *J. Lightwave Technol.*, vol. 16, pp. 991–997, 1998.
[6] Z. Haas and M. A. Santoro, "A mode-filtering scheme for improvement of the bandwidth-distance product in multimode fiber systems," *J. Lightwave Technol.*, vol. 11, pp. 1125–1131, 1993.
[7] L. Raddatz, I. H. White, D. G. Cunningham, and M. C. Nowell, "An experimental and theoretical study of the offset launch technique for the enhancement of the bandwidth of multimode fiber links," *J. Lightwave Technol.*, vol. 16, pp. 324–331, 1998.
[8] R. Olshansky and D. B. Keck, "Pulse broadening in graded-index optical fibers," *Appl. Opt.*, vol. 15, pp. 483–491, 1976. and errata, M. K. Soudagar and A. A. Wali, Appl. Opt., Vol. 32, p. 6678, 1993.
[9] M. J. Adams, D. N. Payne, F. M. E. Sladen, and A. H. Hartog, "Optimum operating wavelength for chromatic equalization in multimode optical fibers," *Electron. Lett.*, vol. 14, pp. 64–66, 1978.
[10] M. J. Yadlowsky and A. R. Mickelson, "Distributed loss and their effects on time-dependent propagation in multimode fibers," *Appl. Opt.*, vol. 32, pp. 6664–6678, 1993.
[11] S. D. Personick, "Baseband linearity and equalization in fiber optic digital communication systems," *Bell Syst. Tech. J.*, vol. 52, pp. 1175–1195, 1973.
[12] G. Yabre, "Comprehensive theory of dispersion in graded-index optical fibers," *J. Lightwave Technol.*, vol. 18, pp. 166–177, Feb. 2000.
[13] J. Gimlett and N. Cheung, "Dispersion penalty analysis for LED/single-mode fiber transmission systems," *J. Lightwave Technol.*, vol. LT-4, pp. 1381–1392, 1986.
[14] E.-G. Neumann, *Single-Mode Fibers*. Berlin, Germany: Springer-Verlag, 1988, pp. 246–247.
[15] D. Gloge, "Optical power flow in multimode fibers," *Bell Syst. Tech. J.*, vol. 51, pp. 1767–1783, 1972.
[16] M. Rousseau and L. Jeunhomme, "Optimum index profile in multimode optical fiber with respect to mode coupling," *Opt. Commun.*, vol. 23, pp. 275–278, 1977.
[17] D. Marcuse, "Coupled mode theory of round optical fibers," *Bell Syst. Tech. J.*, vol. 52, pp. 817–843, 1973.
[18] J. N. Kutz, J. A. Cox, and D. Smith, "Mode mixing and power diffusion in multimode optical fibers," *J. Lightwave Technol.*, vol. 16, pp. 1195–1202, 1998.
[19] R. Olshansky, "Distortion losses in cabled optical fibers," *Appl. Opt.*, vol. 14, pp. 20–21, 1975.
[20] K. Nagano and S. Kawakami, "Measurement of mode conversion coefficients in graded-index fibers," *Appl. Opt.*, vol. 19, pp. 2426–2434, 1980.
[21] J. Saijonmaa, A. B. Sharma, and S. J. Halme, "Selective excitation of parabolic-index optical fibers by Gaussian beams," *Appl. Opt.*, vol. 19, pp. 2442–2453, 1980.
[22] J. Saijonmaa and S. J. Halme, "Reduction of modal noise by using reduced spot excitation," *Appl. Opt.*, vol. 20, pp. 4302–4306, 1981.
[23] M. Rousseau and L. Jeunhomme, "Numerical solution of the coupled-power equation in step-index optical fibers," *IEEE Trans. Microwave Theory Tech.*, vol. MTT-25, pp. 577–585, 1977.
[24] W. Hermann and D. U. Wiechert, "Refractive Index Measurement on PCVD-Bulk Material," Philips Research Laboratories, Aachen, Germany, Intern. Rep., 1988.
[25] S. D. Personick, "Time dispersion in dielectric waveguides," *Bell Syst. Tech. J.*, vol. 50, pp. 843–859, 1971.
[26] A. F. Garito, J. Wang, and R. Gao, "Effects of random perturbations in plastic optical fibers," *Science*, vol. 281, pp. 962–967, 1998.

Gnitabouré Yabre (M'97) was born in Boutaya-P/Zabré, Burkina Faso, in 1962. He received the D.E.A. degree in electronics and the Doctorate degree in optronics, both from the University of Brest, France, in 1989 and 1993, respectively.

From 1989 to 1995, he worked in the RESO Laboratory at the "Ecole Nationale d'Ingénieurs de Brest", France. He is now with COBRA, Interuniversity Research Institute, Eindhoven University of Technology, The Netherlands. During his previous post, his research activities were focused on semiconductor laser nonlinearities, linearization alternatives, injection-locking, subcarrier-multiplexing techniques, fiber-to-wireless communication systems, broad-band optical communication systems and networks. He is currently working mostly on communication multimode optical fibers and related systems.

Dr. G. Yabre has served as a reviewer for the JOURNAL OF LIGHTWAVE TECHNOLOGY, IEEE TRANSACTIONS ON MICROWAVE THEORY AND TECHNIQUES, and *Optics Communications.*